

# Beam-induced backgrounds in the CLIC 3 TeV CM energy interaction region

B. Dalena<sup>1,2</sup>, J. Esberg<sup>2,3</sup> and D. Schulte<sup>2</sup>

1- CEA/SACLAY, DSM/Irfu/SACM - 91191 Gif-sur-Yvette - France

2- CERN - Geneva - Switzerland

3- Department of Physics and Astronomy, Aarhus University, Denmark

Luminosity spectrum and accelerator background levels strongly influence the experimental conditions and have an important impact on detector design. The expected rates of the main beam-beam products at CLIC 3 TeV CM energy, taking into account for machine imperfections, are computed. Among the other machine-induced background the photon fans from the Incoherent Synchrotron Radiation (ISR) photons emitted in the final doublet are evaluated.

## 1 Introduction

In the design of the CLIC interaction region the background levels need to be carefully taken into account, since their rates are expected to be high because of the high energy and high luminosity foreseen. Two main sources of background can be identified: those coming from the beam interactions before and after the collision point, the so called machine backgrounds, and those arising from beam-beam effects, so called beam-beam background. In this paper we review the main beam-beam products in order to give an upper limit to their expected rates, the impact on the luminosity spectrum is also discussed. The distribution of their expected energy and angle are shown. Furthermore we discuss the impact of ISR photons coming from the final doublet on the CLIC interaction region.

Total Luminosity	$[10^{34}\text{cm}^{-2}\text{s}^{-1}]$	5.9
Peak Luminosity	$[10^{34}\text{cm}^{-2}\text{s}^{-1}]$	2.4
repetition freq.	[Hz]	50
bunches/train		312
intra-bunch dist.	[ns]	0.5
particles/bunch	$[10^{10}]$	0.372
bunch length	$[\mu\text{m}]$	44
emittances H/V	[nm]/[nm]	660/20
beam sizes	[nm]/[nm]	45/1

Table 1: CLIC parameters taking into account machine imperfections.

In addition to beamstrahlung photons also QED and QCD backgrounds are produced during collision. The relevant processes are: coherent pair production, incoherent pair production and  $\gamma\gamma \rightarrow$  hadrons events. They are briefly described in the next section. The pairs produced in the coherent processes can contribute to luminosity  $\sim 4\%$  of the total luminosity comes from these pairs mainly in the low energy tail of the spectrum. They can also create collisions where an electron, from a coherent pair produced in the positron beam, collides with the electron beam (and vice versa for a positron). The contribution of these

In order to achieve the required luminosity the two beams at the future linear colliders are focused to very small sizes, see Table 1. In electron-positron collisions the electromagnetic field of each bunch will focus the other, leading to an enhancement of total luminosity (so-called Pinch effect). At the same time due to the strong bending of their trajectory, the beam particles emit high-energy photons (called beamstrahlung photons), which smear the peak of the luminosity spectrum, as shown in Fig. 1.

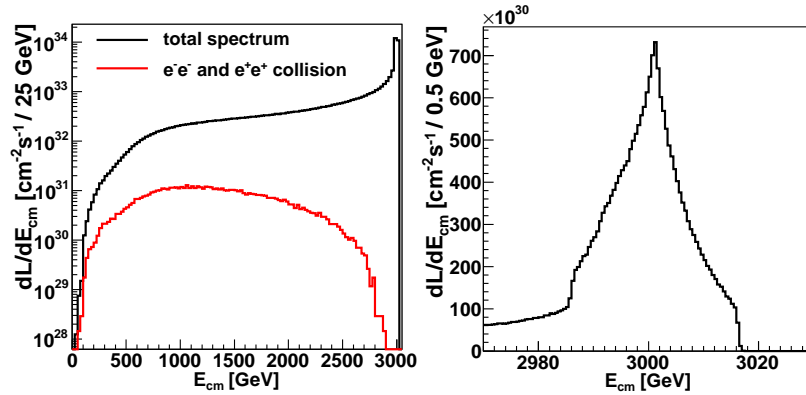


Figure 1: Luminosity spectrum for nominal CLIC 3 TeV CM energy parameters.

type of collisions to the luminosity is  $\sim 1\%$ , which correspond to the red line showed in Fig. 1.

## 2 Beam-Beam backgrounds at 3 TeV CM energy

The beam-beam backgrounds rates are computed using the GUINEA-PIG code [1]. In the simulations we use realistic bunch shapes coming from the full tracking of the two beams in the LINAC and the BDS systems toward the Interaction Point (IP). For this purpose the C++ version of the code [2] has been extensively reviewed and further developed. The beam-beam effects and processes that can be studied by GUINEA-PIG are: emission of beamstrahlung photons, coherent processes such as creation of pairs particles in the strong electromagnetic field of the two bunches, and incoherent processes such as incoherent pairs creation and hadronic events. Other QED processes such as Bhabhas can be simulated as well.

Due to the strong focusing forces generated by the electromagnetic field during interaction, quite a lot of energy goes in the emission of synchrotron radiation photons, so called beamstrahlung photons, generating the long energy tail in the spent beam distribution. On average two beamstrahlung photons are emitted per beam particle. Their energy distribution is peaked at low values but a significant number of them can reach the nominal beam

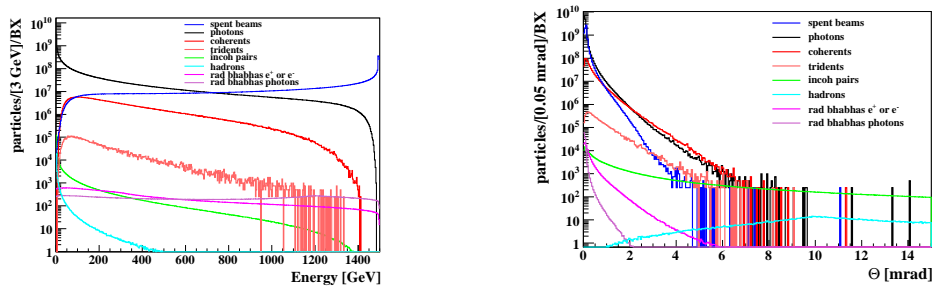


Figure 2: Energy distribution (left) and angular distribution (right) of the particles produced in beam-beam background.

energy, as shown in Fig. 2(left). At CLIC energies, where the beamstrahlung parameter  $\Upsilon$  can be much larger than 0.5, the emitted photons can turn into  $e^+e^-$  pairs by interacting with the collective field of the oncoming beam, so called coherent process. The energy spectrum of the produced pair depends on the beamstrahlung parameter, very low energy pairs are created only for high value of  $\Upsilon$ . The angular distribution is boosted in the direction of the mother particle of the intermediate photon. The red lines in Fig. 2(left) and Fig. 2(right) show their expected energy and angular distribution. In CLIC the coherent pair creation is the dominant process which produces  $e^+e^-$  pairs during collision,  $6.6 \times 10^8$  coherent pairs are expected. Nevertheless at quantum beamstrahlung regime  $\Upsilon > 1$  and for very short bunch length the creation of pair may occur by an intermediate virtual photon, in which case the pair production is said to occur by the trident process. The recent implementation of this process in GUINEA-PIG++ is described in [3], their production in the code follow the one of the coherent pairs, except for the virtuality of the intermediate photon. The expected energy spectrum and their angular distribution for the nominal CLIC beams are shown by the light-red in Fig. 2(left) and Fig. 2(right), respectively. As coherent pairs they follow mainly the beam direction while leaving the interaction region. Their angular distribution is well confined in the 10 *mrad* opening angle of the interaction region beam pipe.

Most of the low energy  $e^+e^-$  pairs are created at the future linear colliders by individual scattering of particles according to three main processes, the so called Breit-Wheeler ( $\gamma\gamma \rightarrow e^+e^-$ ), Bethe-Heitler ( $e^\pm \gamma \rightarrow e^\pm e^+e^-$ ) and Landau-Lifshitz ( $e^+e^- \rightarrow e^+e^-e^+e^-$ ) processes. Their are well known QED processes widely described in standard textbooks [4]. The main formulas implemented in GUINEA-PIG are described in [5]. Their expected rate in CLIC is  $\sim 330 \times 10^3$ , lower then the coherent pair one. Having very low energy, they can be highly deflected in the electromagnetic field of the incoming bunch therefore, they can enter in the detector region. The same process can lead to the production of muon pairs as described in [3], the expected number of muons pair is 12.5 per bunch crossing.

Hadronic events are produced at  $e^+e^-$  colliders through the  $\gamma\gamma \rightarrow$  hadrons reaction. The cross section is known experimentally up to 200 GeV. Different parameterizations of the cross section with the energy are implemented in GUINEA-PIG. According to the one in [6] the expected number of  $\gamma\gamma$  collisions per bunch crossing is 3.2 for a center of mass energy of the two photons of  $> 2$  GeV. The energy distribution of the produced hadrons is peaked at low energy and their angular distribution is more central then the incoherent pairs one, allowing them to reach the central detector region.

$\Delta E/E_{BS}$	29%
$n_\gamma$	2.1 per beam particle
$N_{coherent}$	$66 \times 10^7$
$N_{trident}$	$67 \times 10^5$
$N_{incoherent}$	$330 \times 10^3$
$N_{incoh-muons}$	12.50
$N_{hadrons}$	3.2
$N_{radiative-Bhabhas}$	$110 \times 10^3$

Table 2: Average energy loss due to beamstrahlung and expected beam-beam background rates per bunch crossing for the beam parameters reported in table 1.

Radiative Bhabhas is another well known QED process, in which the binary collision of the electron-positron lead to the emission of a photon in the final state ( $e^+e^- \rightarrow e^+e^- \gamma$ ) [7]. At lowest order the process (in t channel) can be modeled as a two steps reaction: first an  $e^-/e^+$  is substituted by its photon equivalent spectrum, then the compton scattering of the photon on the  $e^+/e^-$  is calculated. The expected rate at CLIC is  $\sim 110 \times 10^3$ . The energy and angular distributions of the scattered  $e^-/e^+$  and photon are shown by the pink and light-pink curve in Fig. 2(left) and Fig. 2(right). Their

energy is spread over a wide range (from 0 up to the nominal beam energy). Their angular distributions are mainly peaked in the very forward direction.

All the expected beam-beam background rates we have studied are summarized in Table 2. The emittance values considered in the simulations include the budgets for imperfections. The actual values depend on the single machine and change during operation.

## 2.1 Machine imperfections and background rates

If machine imperfections are well controlled the final emittance of the two beams can be lower than the one reported in Table 1, leading to a high luminosity and high background rate. The overall correlation of the background rates with the horizontal and vertical emittance of the two beams has been studied in [8]. In the following we report the evaluation of an upper limit of the rate of the two backgrounds of interest for the detectors, such as incoherent pairs and hadronic events. For this purpose we track the two beams in the Main LINAC and the BDS considering realistic imperfections and nominal beam parameters at the entrance of the LINAC, using the tracking code PLACET [9]. We consider here machine imperfections in the vertical plane only, which is the most critical one due to the very small emittance. The vertical emittance at the entrance of the main LINAC is 10 nm and the machine imperfections considered in the simulation are reported in Table 3.

imperfections	dim.	value
BPM vert. offset	$\mu\text{m}$	14
BPM resolution	$\mu\text{m}$	0.1
accelerating structure vert. offset	$\mu\text{m}$	7
accelerating structure vert. tilt	$\mu\text{rad}$	142
quadrupole vert. offset	$\mu\text{m}$	17
quadrupole vert. roll	$\mu\text{rad}$	100
beam parameters	dim.	value
Bunch charge N	particles	3.72e+09
Bunch length $\sigma_z$	$\mu\text{m}$	44
hor. emittance $\gamma\epsilon_x$	nm	660
vert. emittance $\gamma\epsilon_y$	nm	10

Table 3: Values of the machine imperfections and beam parameters used in the main LINAC simulations.

These imperfections are enough to bring the vertical emittance of the nominal beams to growth up to several order of magnitude if no correction scheme is applied to the machines. When the Beam-Based-Alignment (BBA), described in [10], is applied to the machines the average emittance growth at the end of the ML stays well below five nm, which is the budget for static imperfections in the main LINAC. We steer the beams coming from the corrected linacs into the BDS, and track them to the IP, without any imperfections in the BDS. The bunch shapes, so obtained, are used to compute luminosity and background rates again. This procedure allow us to evaluate the effect of imperfections in the Main Linac only on the luminosity and on the background rates. Moreover since further machine imperfections in the BDS would only lower the luminosity and background rates, this assumption ensure that we estimate a maximum value for the background rates.

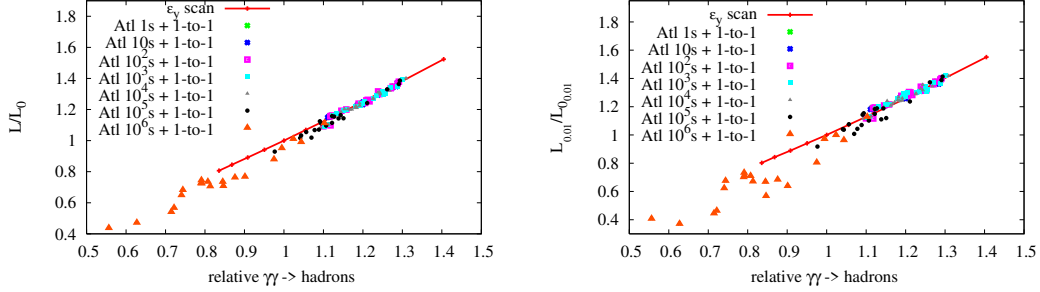


Figure 3: Total luminosity  $L$ (left) and Peak luminosity  $L_{0.01}$ (right) vs number of  $\gamma\gamma \rightarrow$  hadrons events, normalized to the nominal values, for perfect machines and different vertical emittance values, and for corrected machines and nominal vertical emittance.

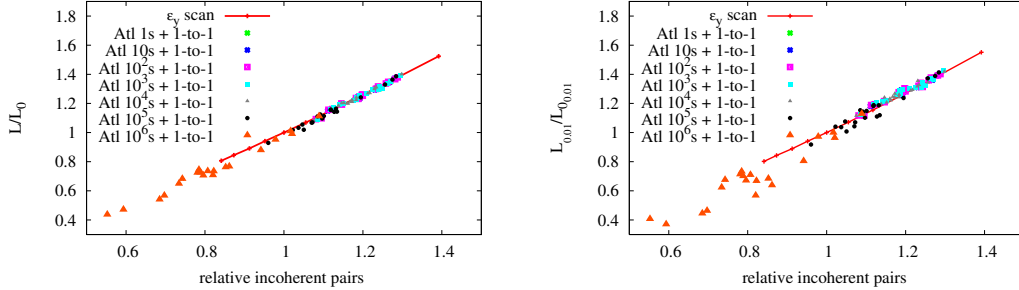


Figure 4: Total luminosity  $L$ (left) and Peak luminosity  $L_{0.01}$ (right) vs number of incoherent pairs events, normalized to the nominal values, for perfect machines and different vertical emittance values, and for corrected machines and nominal vertical emittance.

The cases of perfect machines and scaled beam emittances, as in Figs. 3 and 4 are compared with the cases of corrected machines and initial nominal beam parameters. The Total and Peak luminosities are shown in separated plots. We define Peak Luminosity the luminosity contained into  $\pm 1\%$  around the 3 TeV CM peak.

The correlation between luminosity and background rates variations is linear for both the background types considered, and it stays linear for both total( $L$ ) and peak( $L_{0.01}$ ) luminosity. The fluctuation in the variation of luminosity and background rates for the corrected machines is on average  $\sim 5\%$ , indicating that different emittance values can be reached by the different machines after the linac BBA correction. In these simulations the mean luminosity reached by the corrected machines is about 30% higher than the values reported in Table 1, and on average 25% more background with respect to the values in Table 2. When  $10^6$  s of ground motion is applied to the Main LINAC the luminosity and background rates start to fluctuate more around the linear behavior (the fluctuations of the background rates are  $> 15\%$ ). The majority of the machines have a relative low luminosity while still a significant number of hadronic events and incoherent pairs can be produced. Even though the background rates stay below the values quoted in Table 2. A safety margin of 50% more luminosity and 40% more background (for both hadronic events and incoherent pairs) can

be defined. Detectors should thus be able to handle this level in order not to have to reduce luminosity to reduce background.

### 3 Synchrotron Radiation photons from the final doublet

In order to provide an acceptable cleaning efficiency of the desired beam halo the collimation apertures are determined from the following conditions:

1. minimize the synchrotron radiation photons emitted in the first final quadrupole magnet which can hit the 2nd final quadrupole (QD0);
2. minimize the beam particles that can hit either QF1 or QD0.

Macroparticles with high transverse amplitude are tracked using the code PLACET [9], taking into account the emission of synchrotron radiation and all the non linear elements of the system. The particles positions and angles have been checked at the entrance, in the middle and at the exit of QF1 and QD0. The dangerous particles are efficiently removed for collimator apertures of  $< 15 \sigma_x$  in the horizontal plane and of  $< 55 \sigma_y$  in the vertical plane. Therefore we define  $15 \sigma_x$  and  $55 \sigma_y$  as the collimation depths [11].

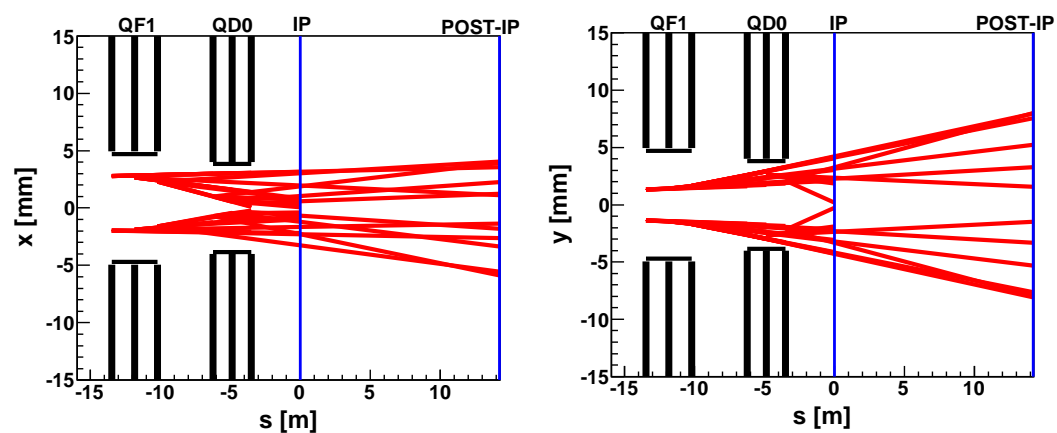


Figure 5: Incoherent Synchrotron radiation photon fans at 3 TeV.

Fig. 5 shows the residual synchrotron radiation fans from the final quadrupoles QF1 and QD0 to the IP for an envelop covering 15 and 55 standard deviations in  $x$  and in  $y$ , respectively. At the IP the photon cone is inside a cylinder of radius of five mm, which is well inside the beam pipe aperture. Therefore, in principle, they are not an issue of concern for the detectors.

The distribution of the expected energy of the radiated photons in the final doublet for a perfect machine and nominal beam parameters is shown in Fig. 6. The spectrum is peaked at very low energy, i.e.  $< 1$  MeV, with an energy tail up to  $\sim 1$  GeV. The number of radiated photons is  $\sim 1$  for beam particle. An internal shielding of the beam pipe in the final doublet magnets region should be foreseen.

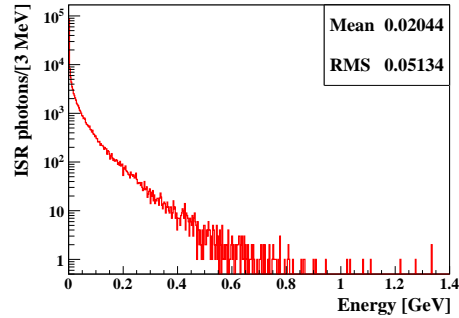


Figure 6: Energy of synchrotron radiation photons emitted in the final doublet.

## 4 Conclusion

Beam-beam effects at CLIC 3 TeV CM energy have been reviewed. The expected production rates, their energy and angular distribution evaluated. A safety margin of 40% of the background processes of interest for the detectors is estimated. The ISR photon fans coming from the final doublet is shown to be well inside the beam pipe aperture at the IP, considering the nominal collimation depths. Their energy distribution is peaked at few MeV.

## References

- [1] D. Schulte, *Beam-Beam Simulations with GUINEA-PIG*, ICAP98, Monterey, CA, USA (1998).
- [2] G. Le Meur *et al.*, *Description of GUINEAPIG++, the C++ upgraded version of the GUINEA-PIG beam-beam simulation program*, EUROTeV-Report-2008-067.
- [3] J. Esberg, *Simulations of the interaction point for the TeV-scale  $e^+e^-$  colliders* IPAC'11 proceeding.
- [4] for example: V.B. Berestetskii, E.M. Lifshitz and L.P. Pitaevskii, *Relativistic Quantum Theory*, Pergamon Press (1971).
- [5] D. Schulte, *Study of the Electromagnetic and Hadronic Background in the Interaction Region of the TESLA Collider*, PhD-thesis, TESLA 97-98(1997).
- [6] G.A. Schuler and T. Sjostrand, *gamma-gamma Physics at Linear Colliders*, CERN-TH/96-119 (1996).
- [7] D.A. Karlen, *A Study of low  $Q^2$  radiative bhabha scattering*, PhD-thesis, SLAC-235 (1988).
- [8] B. Dalena and D. Schulte, *Beam-Beam background in CLIC in presence of imperfections*, IPAC10, Kyoto, Japan (2010).
- [9] D. Schulte *et al.*, *Simulation Package based on PLACET*, CERN/PS, 2001/028.
- [10] D. Schulte, *Beam-based alignment in the new CLIC main linac*, PAC09, Vancouver, Canada (2009).
- [11] J. Resta Lopez *et al.* *Status report of the baseline collimation system of CLIC*, arXiv:1104.2426 and arXiv:1104.2431.